Available online at www.sciencedirect.com
SCIENCE DIRECT®
Journal of Power Sources 119–121 (2003) 216–220
JOURNAL OF POWER SOURCES
www.elsevier.com/locate/jpowsour

The electrochemical behavior of $xLiNiO_2 \cdot (1-x)Li_2RuO_3$ and $Li_2Ru_{1-y}Zr_yO_3$ electrodes in lithium cells

Gregory J. Moore*, Christopher S. Johnson, Michael M. Thackeray

Electrochemical Technology Program, Chemical Technology Division, Argonne National Laboratory, Argonne, IL 60439, USA

Abstract

Cathode materials derived from Li_2RuO_3, Li_2ZrO_3 and $LiNiO_2$ have been evaluated in lithium cells at room temperature as part of an ongoing study of composite $xLiMO_2 \cdot (1-x)Li_2M'O_3$ electrodes. Our results confirm previous reports that two lithium ions can be initially extracted from Li_2RuO_3, but that only one lithium ion can be cycled between 4.4 and 2.8 V with a rechargeable capacity of approximately 200 mAh/g. Extending the voltage window to 4.6–1.4 V increases the reversible capacity of the Li_2RuO_3 electrode significantly, to nearly 300 mAh/g. Similar capacities are obtained from a Zr-substituted electrode, $Li_2Ru_{1-y}Zr_yO_3$ for $y = 0.1$, with excellent cycling stability. A composite electrode, $0.7LiNiO_2 \cdot 0.3Li_2RuO_3$, provides a steady 150 mAh/g when cycled between 4.6 and 2.7 V.

Keywords: Lithium cell; Electrode; Li_2RuO_3; Lithium ruthenate

1. Introduction

Layered metal oxide electrodes in the family of $LiMO_2$ compounds (M = Co, Ni, Mn) are limited in their electrochemical performance by phase transformations that occur during the extraction of lithium—for example, by the migration of the M ions into the lithium layers or by surface reactions with the electrolyte. In attempts to stabilize these $LiMO_2$ electrodes at high potentials versus lithium, efforts have been made to fabricate "composite" electrodes consisting of an electrochemically inactive $Li_2M'O_3$ component (M′ = Ti, Zr, Mn) and an electrochemically active $LiMO_2$ component by exploiting the strong similarity that exists between their structures [1–5]. Thus far, this approach has been successful in improving the coulombic efficiency and structural stability of electrodes such as $xLiMn_{0.5}Ni_{0.5}O_2 \cdot (1-x)Li_2TiO_3$ ($0.7 < x < 1.0$) when lithium cells are charged and discharged over a wide potential window [6,7].

Li_2RuO_3 is another example of a $Li_2M'O_3$ compound but in this case the Ru atoms are electrochemically active because lithium can be extracted from Li_2RuO_3 with the concomitant oxidation of ruthenium from a tetravalent to hexavalent state. In this respect, it has already been demonstrated that both lithium ions can be extracted from Li_2RuO_3 but that only one lithium ion can be cycled repeatedly [8,9]. Therefore, an electrochemically active Li_2RuO_3 component offers the possibility of contributing not only to the stability of composite $xLiMO_2 \cdot (1-x)Li_2M'O_3$ electrodes, but also to their capacity. Because ruthenium is a relatively heavy element compared with the first-row transition metals, Li_2RuO_3 also offers a significantly higher theoretical volumetric capacity (999 mAh/ml) compared with $LiMO_2$ electrodes (M = Mn, Co, Ni), which for $LiNiO_2$ is 785 mAh/ml. Furthermore, Li_2RuO_3 has semiconducting properties with low resistivity that make it attractive as an insertion electrode [10]. Therefore, Li_2RuO_3 has structural, electrical and electrochemical properties that, if successfully exploited, may result in specialized high energy/power sources when materials costs can be justified.

In this paper, we report electrochemical data of (1) a substituted $Li_2Ru_{1-y}Zr_yO_3$ electrode ($y = 0.1$) and (2) a "composite" electrode in the $xLiNiO_2 \cdot (1-x)Li_2RuO_3$ system in which $x = 0.7$. These data are compared with the performance of standard Li_2RuO_3 electrodes over a high voltage range, typically 4.5–2.8 V, and over a wider operating voltage window, typically 4.5–1.4 V.

2. Experimental

Li_2RuO_3 was prepared following the method described by Kobayashi et al. [9]. $RuO_2 \cdot xH_2O$ was dried in an evacuated oven in a helium glovebox at 120 °C for 8 h to remove the crystal water. Thereafter, it was ground together with

* Corresponding author.
E-mail address: thackeray@cmt.anl.gov (G.J. Moore).

0378-7753/03/$ – see front matter
doi:10.1016/S0378-7753(03)00184-8

Li_2CO_3 (5% excess) and fired at 950 °C for 24 h in an oxygen atmosphere.

$LiNiO_2$ and a composite electrode $xLiNiO_2 \cdot (1-x)$-Li_2RuO_3 ($x = 0.7$) were synthesized by (1) dissolving the appropriate quantities of $LiNO_3$, $Ni(NO_3)_2 \cdot 6H_2O$ and $Ru(NO)(NO_3)_3$ in water (1.5% w/v), (2) evaporating the solutions, while stirring, to dryness, and (3) heating the product to 450 °C for 4 h to drive off NO_x gases. The resulting powder was ground, pressed into a pellet, and heated to 750 °C in oxygen for 15 h.

The substituted $Li_2Ru_{1-y}Zr_yO_3$ compound was synthesized by the Pechini method [11] using precursor solutions of $LiNO_3$, $ZrO(NO_3)_2$ and $Ru(NO)(NO_3)_3$ (1.5% w/v in water) with 1 eq. of citric acid for every 2 eq. metal ions, and 3 eq. of ethylene glycol for every 2 eq. of citric acid. After dissolving the metal nitrates in water, citric acid was added as a complexing agent. The resulting solution was heated, while it was stirred, and the ethylene glycol added when almost all the solvent had evaporated. After combustion on a hot plate, the finely divided powder was ground, pressed into a pellet, and sintered at 950 °C in oxygen for 24 h. Powder X-ray diffraction patterns of the products were obtained with a Siemens D5000 diffractometer between 5 and 80° 2θ at a scan rate of 1°/min.

Electrode laminates were prepared from a mixture of carbon, active material and polyvinylidine difluoride (PVDF) binder in the following proportions by weight: 4% acetylene black, 4% SFG-6 carbon, 84% active material, and 8% PVDF dissolved in *n*-methylpyrolidinone (NMP, 12 wt.% solution). After grinding the electrode components, additional NMP was added to form a thick slurry that was then cast onto 10.1 μm thick aluminum foil. After the NMP was evaporated at 70 °C overnight, the laminate was dried further at 80 °C in a vacuum oven for 6 h. The porosity of the laminate was approximately 35%.

Electrochemical tests were performed on two-electrode button cells, size 2032. The metallic lithium anode and laminated metal oxide cathode were punched out as discs, each of 9/16 in. diameter, and were insulated from one another by a porous Celgard 2500 separator. The electrolyte was 1 M $LiPF_6$ in EC:DEC (1:1 solvent mixture, LP40, Merck Industries). Approximately 7 mg of active material was used in each cathode. Cell cycling was controlled with a Maccor battery cycler. Cells were charged and discharged between predetermined voltage limits at a constant current rate of 0.1 mA/cm^2.

3. Results and discussion

The powder X-ray diffraction patterns of $LiNiO_2$, $0.7LiNiO_2 \cdot 0.3Li_2RuO_3$, Li_2RuO_3 and $Li_2Ru_{0.9}Zr_{0.1}O_3$ are shown in Fig. 1a–d, respectively. $LiNiO_2$ has a layered structure with trigonal symmetry (space group *R*-3*m*). Although Li_2RuO_3 and Li_2ZrO_3 have monoclinic symmetry (C2/c), they can be considered to be isostructural with $LiNiO_2$ because they are layered compounds in which the cation distribution can be represented as $Li(Li_{0.33}M_{0.67}')O_2$; there is, therefore, a strong structural relationship between layered $LiMO_2$ and $Li_2M'O_3$ compounds, which allows for the possibility of synthesizing composite structures in which domains of $LiMO_2$ and $Li_2M'O_3$ with a common closely packed oxygen array can be crystallographically connected. Structure analyses of such composite electrodes, for example, $Li_{1.2}Mn_{0.4}Cr_{0.4}O_2$ (or $0.4LiCrO_2 \cdot 0.4Li_2MnO_3$) have provided support for this hypothesis [2,4]. Fig. 1b shows that the composite $0.7LiNiO_2 \cdot 0.3Li_2RuO_3$ electrode keeps the predominant symmetry of the parent $LiNiO_2$ structure, whereas the Zr-substituted $Li_2Ru_{0.9}Zr_{0.1}O_3$ electrode maintains monoclinic symmetry, as expected.

A schematic illustration of a ''structural phase diagram'', in which the compositional changes that occur in $LiMO_2$, $Li_2M'O_3$ and composite $xLiMO_2 \cdot (1-x)Li_2M'O_3$ electrodes can be followed, is shown in Fig. 2. In this three-dimensional diagram, which has at its apices $LiMO_2$, MO_2, $Li_2M'O_3$ and $M'O_3$, the composition of $LiMO_2$ electrodes, such as $LiCoO_2$ or $LiNiO_2$, varies in one dimension along the $LiMO_2$–MO_2 tie-line (edge) of the phase diagram as lithium

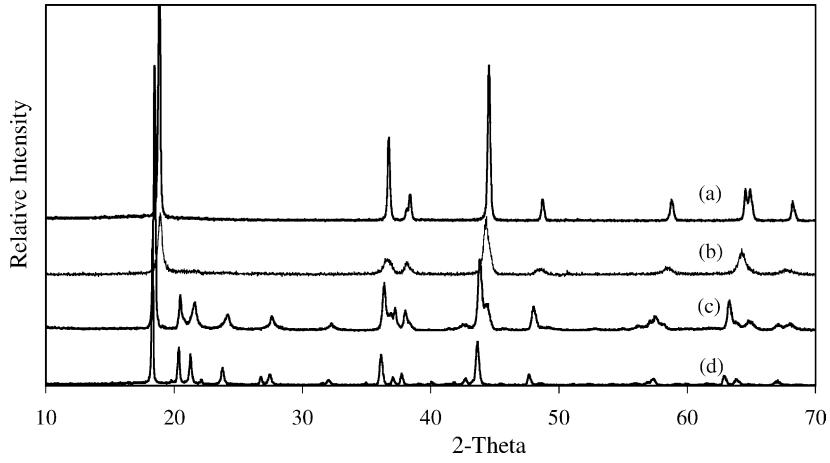

Fig. 1. X-ray diffraction patterns of (a) $LiNiO_2$; (b) $0.7LiNiO_2 \cdot 0.3Li_2RuO_3$; (c) Li_2RuO_3; and (d) $Li_2Ru_{0.9}Zr_{0.1}O_3$.

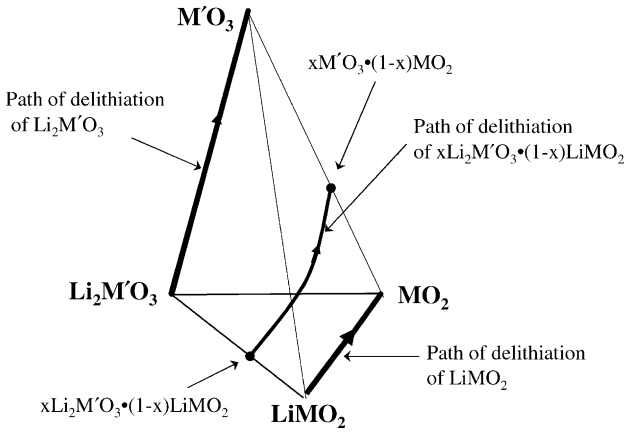

Fig. 2. Schematic illustration of a "structural phase diagram" showing the path of Li extraction/insertion with $LiMO_2$, $Li_2M'O_3$ and composite $xLiMO_2{\cdot}(1-x)Li_2M'O_3$ electrodes.

is electrochemically extracted from, and reinserted into, the structure during charge and discharge. Similarly, the composition of an electrochemically active $Li_2M'O_3$ electrode, such as Li_2RuO_3, varies along the $Li_2M'O_3$–$M'O_3$ tie-line (edge) of the phase diagram. For a composite $xLiMO_2{\cdot}(1-x)Li_2M'O_3$ electrode in which both components are electrochemically active, the composition of the electrode can vary in three dimensions within the pyramid of the phase diagram from one tie-line to another, as shown by the dotted line in Fig. 2.

Fig. 3a shows the voltage profiles of the 1st, 10th, and 20th charge/discharge cycles of a Li/Li_2RuO_3 cell between 4.4 and 2.8 V. On the initial charge, a capacity of 310 mAh/g was drawn from the Li_2RuO_3 electrode, which corresponded to 94% of its theoretical value (329 mAh/g). Although 245 mAh/g was recovered on the first discharge (i.e. 79% of the initial charge capacity), repeated cycling showed a steady decrease in discharge capacity that stabilized when it reached approximately 190 mAh/g (Fig. 3a). Kobayashi et al. [9] have reported a rechargeable capacity of approximately

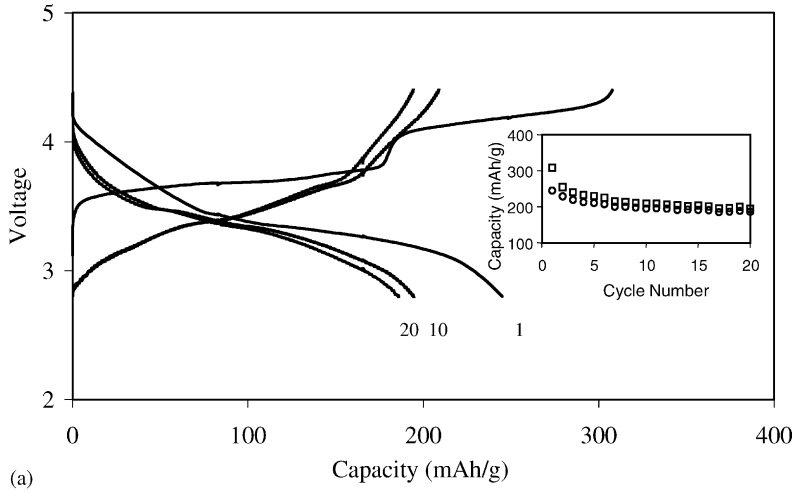

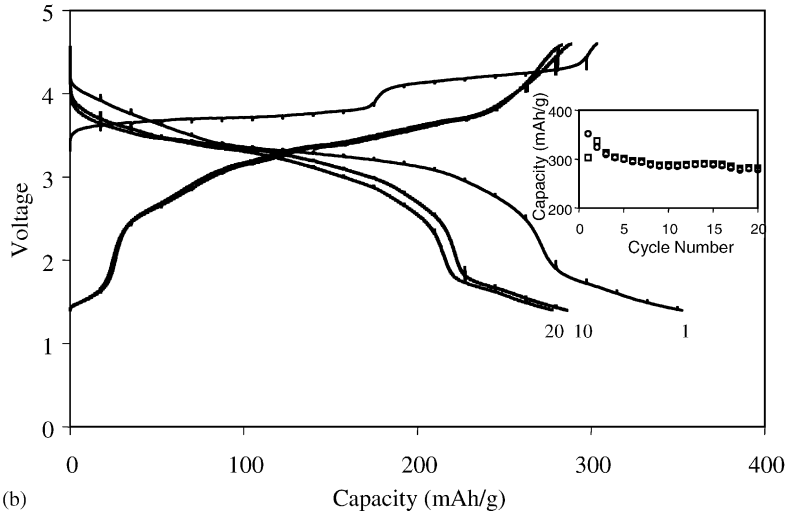

Fig. 3. Voltage profiles of Li/Li_2RuO_3 cells cycled between (a) 4.4 and 2.8 V, and (b) 4.6 and 1.4 V. Capacity vs. cycle number plots are provided as insets. (□) Charge and (○) discharge.

150 mAh/g when Li_2RuO_3 electrodes are cycled between 3.0 and 4.0 V. These authors attributed the electrochemical process between 3.0 and 4.0 V to a reversible phase transition from the rocksalt Li_2RuO_3 structure to $Li_{0.9}RuO_3$ with an ilmenite-type structure. Our data show that the higher voltage reaction that occurs between 4.0 and 4.4 V is irreversible, suggesting that the structure of the electrode changes significantly at this high potential to yield a "conditioned" electrode.

In an attempt to recover the lost capacity described above, the voltage window of the Li/Li_2RuO_3 cells was widened to 4.6–1.4 V. Significant capacity was recovered from the electrode, in two stages: (1) between 2.8 V (i.e. the lower cut-off voltage in Fig. 3a) and 1.8 V, and (2) between 1.8 and 1.4 V, with good reversibility. After the initial conditioning of the electrode (two cycles), the Li_2RuO_3 electrode delivered a capacity close to 300 mAh/g for the next 18 cycles. Although further work is required to determine the exact reaction mechanism that occurs within $Li_{2-x}RuO_3$ electrodes, the voltage profiles suggest that the additional capacity between 2.8 and 1.8 V may be attributed to the continued insertion of lithium into the conditioned $Li_{2-x}RuO_3$ electrode structure. It is proposed that the capacity obtained between 1.8 and 1.4 V occurs by further insertion to yield a layered $Li_{2+y}RuO_3$ structure, similar to the formation of layered Li_2MO_2 phases that have been reported on lithiating $LiMn_{0.5}Ni_{0.5}O_2$ electrodes [6,7], with the possibility of some Ru extrusion at the particle surface near 1.4 V.

The charge/discharge profiles of a lithium cell with a Zr-substituted $Li_2Ru_{0.9}Zr_{0.1}O_3$ electrode, when cycled between 4.3 and 2.7 V, are shown in Fig. 4a. Apart from the initial cycle, during which there was an appreciable capacity loss, this Zr-substituted electrode performed with significantly greater cycling stability and superior coulombic efficiency than did the parent Li_2RuO_3 electrode (Fig. 3a), delivering a steady 200 mAh/g; the slight fluctuation in the capacity versus cycle number plot (Fig. 4a) is attributed to variations in the room temperature of the laboratory in which the tests were conducted. Opening the voltage window of this cell to 4.6–1.2 V resulted in a discharge capacity near 300 mAh/g

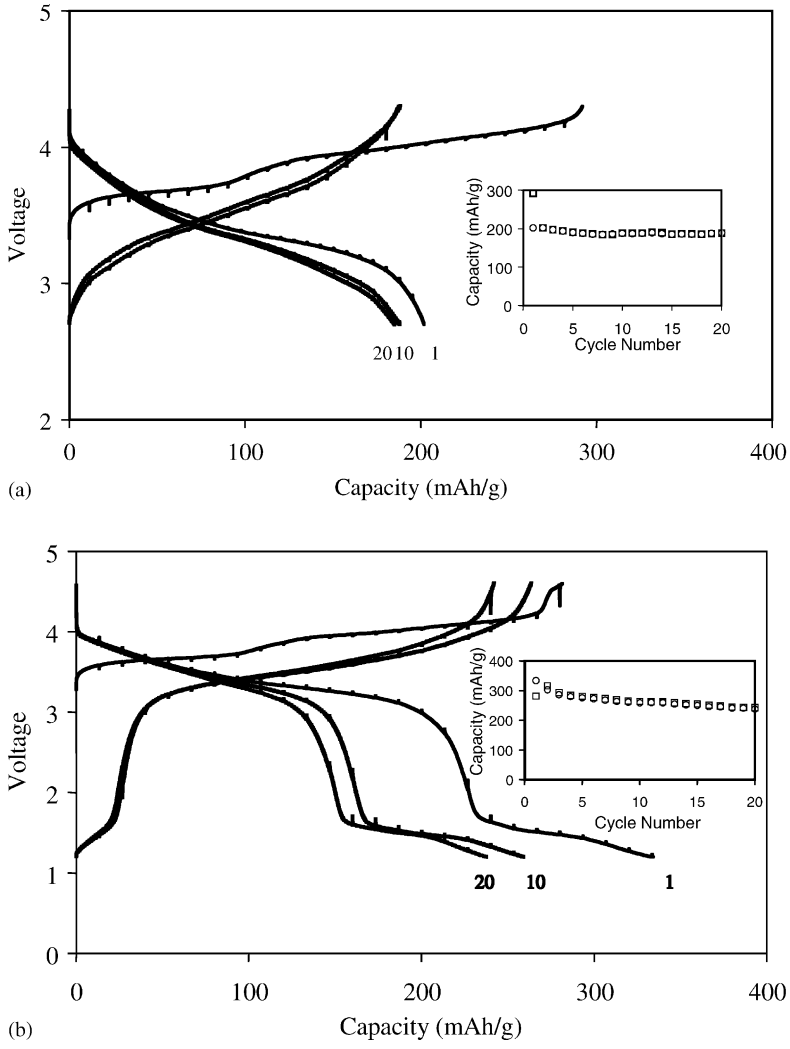

Fig. 4. Voltage profiles of Li/$Li_2Ru_{0.9}Zr_{0.1}O_3$ cells cycled between (a) 4.3 and 2.8 V and (b) 4.6 and 1.2 V. Capacity vs. cycle number plots are provided as insets. (□) Charge and (○) discharge.

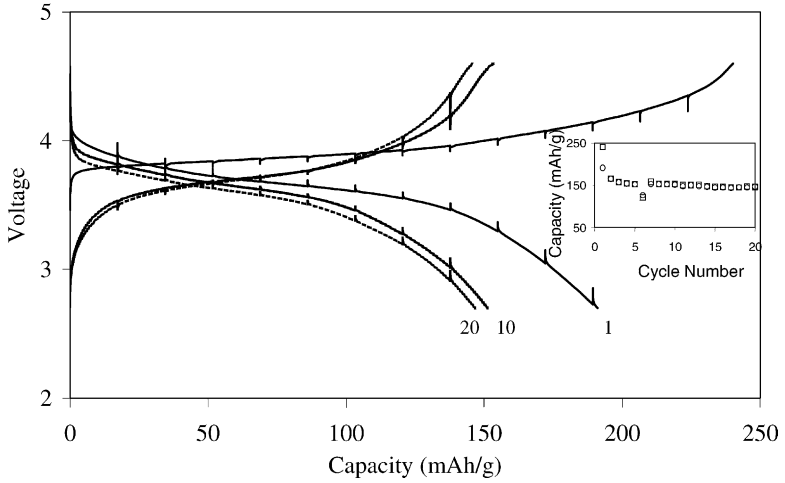

Fig. 5. Voltage profiles of $Li/0.7LiNiO_2{\cdot}0.3Li_2RuO_3$ cells cycled between 4.6 and 2.7 V. Capacity vs. cycle number plots are provided as insets. (□) Charge and (○) discharge.

(Fig. 4b). Although these cells operated with excellent coulombic efficiency, they lost capacity more rapidly than cells with the parent Li_2RuO_3 electrode (Fig. 3a). This phenomenon was attributed to the lower end voltage of the $Li/Li_2Ru_{0.9}Zr_{0.1}O_3$ cell (1.2 V) compared with the Li/Li_2RuO_3 cell (1.4 V), and to a greater amount of (irreversible) Ru extrusion, as manifested by the steady decrease in capacity delivered by the $Li_2Ru_{0.9}Zr_{0.1}O_3$ electrode between 1.4 and 1.2 V versus Li on prolonged cycling (Fig. 4b).

The electrochemical behavior of a $Li/0.7LiNiO_2{\cdot}0.3Li_2RuO_3$ cell when cycled between 4.6 and 2.7 V is shown in Fig. 5. As with Li_2RuO_3 and $Li_2Ru_{0.9}Zr_{0.1}O_3$ electrodes, the first charge/discharge cycle is coulombically inefficient; thereafter, these electrodes yield a steady capacity of 150 mAh/g. The voltage profiles of $Li/0.7LiNiO_2{\cdot}0.3Li_2RuO_3$ cells do not show the inflections that are characteristic of the small but significant phase transitions in the parent $LiNiO_2$ electrode that affect its electrochemical performance; the absence of these phase transitions is consistent with many other compositionally modified $LiNiO_2$ electrodes that show enhanced electrochemical performance and stability compared with pure $LiNiO_2$ [12,13].

4. Conclusions

It has been demonstrated that $Li_2M'O_3$ rock salt structures play an important role in the electrochemical behavior and stability of layered insertion electrodes for lithium batteries. When electrochemically inactive $Li_2M'O_3$ components such as Li_2ZrO_3 are incorporated as a solid solution into a second, isostructural component such as Li_2RuO_3 or a layered $LiMO_2$ component such as $LiNiO_2$, electrochemical capacities of approximately 200 mAh/g can be achieved within a high voltage range (~4.5–2.8 V). The reversible capacity can be increased to 300 mAh/g if the end voltage is lowered to 1.4 V; however, cycle life is compromised by an apparent structural degradation of the electrode if cells are discharged to lower potentials.

Acknowledgements

Financial support from the DCI post-doctoral fellowship program is greatly appreciated.

References

[1] C.S. Johnson, S.D. Korte, J.T. Vaughey, M.M. Thackeray, T.E. Bofinger, Y. Shao-Horn, S.A. Hackney, J. Power Sources 81/82 (1999) 491.
[2] B. Ammundsen, J. Paulsen, Adv. Mater. 13 (2001) 943.
[3] C.S. Johnson, M.M. Thackeray, The Electrochem. Soc. Inc., Proc. PV 2000-36 (2001) 47.
[4] B. Ammundsen, J. Paulsen, I. Davidson, R.S. Liu, C.-H. Shen, J.-M. Chen, L.-Y. Jang, J.-F. Lee, J. Electrochem. Soc. 149 (2002) A431.
[5] J.-S. Kim, C.S. Johnson, M.M. Thackeray, Electrochem. Commun. 4 (2002) 205.
[6] C.S. Johnson, J.-S. Kim, A.J. Kropf, A.J. Kahaian, J.T. Vaughey, M.M. Thackeray, Electrochem. Commun. 4 (2002) 492.
[7] C.S. Johnson, J.-S. Kim, A.J. Kropf, A.J. Kahaian, J.T. Vaughey, M.M. Thackeray, Chem. Mater., in press.
[8] A.C.W.P. James, J.B. Goodenough, J. Solid State Chem. 74 (1988) 287.
[9] H. Kobayashi, R. Kanno, Y. Kamamoto, M. Tabuchi, O. Nakamura, M. Takano, Solid State Ionics 82 (1995) 25.
[10] H. Kobayashi, R. Kanno, Y. Kamamoto, M. Tabuchi, O. Nakamura, Solid State Ionics 86–88 (1996) 859.
[11] M.P. Pechini, US Patent 3,330,697 (1967).
[12] Y.A. Gao, M.V. Yakovleva, W.B. Ebner, Electrochem. Solid State Lett. 1 (1998) 117.
[13] J. Kim, K. Amine, Electrochem. Commun. 3 (2001) 52.